**University of Dayton**
**eCommons**

Chemical and Materials Engineering Faculty Publications

Department of Chemical and Materials Engineering

2010

# Electrostatic Quadrupole Plasma Mass Spectrometer Measurements during Thin Film Depositions using Simultaneous Matrix Assisted Pulsed Laser Evaporation and Magnetron Sputtering

Chad N. Hunter
*Air Force Research Laboratory*

Michael H. Check
*Universal Technology Co.*

Christopher Muratore
*University of Dayton*, cmuratore1@udayton.edu

Andrey A. Voevodin
*Air Force Research Laboratory*

Follow this and additional works at: https://ecommons.udayton.edu/cme_fac_pub

🔵 Part of the Other Chemical Engineering Commons, Other Materials Science and Engineering Commons, and the Polymer and Organic Materials Commons

# Electrostatic quadrupole plasma mass spectrometer measurements during thin film depositions using simultaneous matrix assisted pulsed laser evaporation and magnetron sputtering

C. N. Hunter[a)]
*Materials and Manufacturing Directorate, Air Force Research Laboratory, 2941 Hobson Way,*
*Wright-Patterson AFB, Ohio 45433-7750*

M. H. Check
*Universal Technology Corporation, 1270 North Fairfield Road, Dayton, Ohio 45532*

C. Muratore and A. A. Voevodin
*Materials and Manufacturing Directorate, Air Force Research Laboratory, 2941 Hobson Way,*
*Wright-Patterson AFB, Ohio 45433-7750*

A hybrid plasma deposition process, combining matrix assisted pulsed laser evaporation (MAPLE) of carbon nanopearls (CNPs) with magnetron sputtering of gold was investigated for growth of composite films, where 100 nm sized CNPs were encapsulated into a gold matrix. Composition and morphology of such composite films was characterized with x-ray photoelectron spectroscopy, scanning electron microscopy, and transmission electron microscopy (TEM) analysis. Carbon deposits on a gold magnetron sputter target and carbon impurities in the gold matrices of deposited films were observed while codepositing from gold and frozen toluene-CNP MAPLE targets in pure argon. Electrostatic quadrupole plasma analysis was used to determine that a likely mechanism for generation of carbon impurities was a reaction between toluene vapor generated from the MAPLE target and the argon plasma originating from the magnetron sputtering process. Carbon impurities of codeposited films were significantly reduced by introducing argon-oxygen mixtures into the deposition chamber; reactive oxygen species such as O and O+ effectively removed carbon contamination of gold matrix during the codeposition processes. Increasing the oxygen to argon ratio decreased the magnetron target sputter rate, and hence hybrid process optimization to prevent gold matrix contamination and maintain a high sputter yield is needed. High resolution TEM with energy dispersive spectrometry elemental mapping was used to study carbon distribution throughout the gold matrix as well as embedded CNP clusters. This research has demonstrated that a hybrid MAPLE and magnetron sputtering codeposition process is a viable means for synthesis of composite thin films from premanufactured nanoscale constituents, and that cross-process contaminations can be overcome with understanding of hybrid plasma process interaction mechanisms. © *2010 American Vacuum Society.* [DOI: 10.1116/1.3372401]

## I. INTRODUCTION

Matrix-assisted pulsed laser evaporation (MAPLE) is a physical vapor deposition technique in which thin films of nanostructured organic or inorganic materials (e.g., polymer molecular clusters, carbon nanotubes and nanopearls, DNA nanostructures, etc.) are deposited using a pulsed laser to evaporate a frozen target consisting of these nanostructured materials dissolved in a volatile solvent matrix.[1–4] The laser pulses sublimate the solvent and heat the solute material, causing it to be ejected from the target surface along with the solvent vapor. A coating from the solute material is formed on the substrate surface, while the volatile solvent molecules are evacuated from the deposition chamber.[1] The advantage of using MAPLE compared to other laser techniques, such as pulsed laser deposition, is that diverse solute materials, such as nanoparticles, nanotubes, or large molecule structures can be deposited while sustaining little or no damage during the

process.[1–4] The process then offers an opportunity to produce films of various nanostructured constituents, which are of the interest to electronics, sensors, biomedical, tribological, and other engineering applications. The MAPLE process could be enhanced further if such nanostructures could be simultaneously embedded in metal, ceramic, or polymer matrices, which requires MAPLE combination with other thin film deposition techniques.

Recently, optimization studies for depositing carbon nanopearls (CNPs) using MAPLE were performed.[5] These studies established correlations between the morphology of deposited carbon nanopearl films and matrix solvents, laser energy, repetition rate, background pressure, and substrate temperature. It was also demonstrated that hybrid films of carbon nanopearls embedded in gold matrices could be synthesized by codepositing CNPs using MAPLE and gold using magnetron sputtering. However, carbon impurities were present in the films due to the interactions of toluene molecules with the magnetron plasma. Carbon-based solvents

---
a)Electronic mail: chad.hunter@wpafb.af.mil

are advantageous for MAPLE processing due to their volatility and laser absorption coefficients,[6] but the impurities resulting from the interactions of toluene vapor with the argon plasma can limit the physical characteristics of synthesized films. The focus of the current work was (1) to understand the effects of MAPLE and magnetron sputtering codeposition conditions on neutral and ionic species present during the process, (2) to determine mechanisms for generation of carbon impurities in deposited films, and (3) to propose effective methodologies for reducing the impact of these impurities when using hybrid plasma processes for embedding CNP nanostructures in metal matrices.

## II. EXPERIMENT

Carbon nanopearls synthesized using a chemical vapor deposition process[7] were obtained for this study. Briefly, the nanopearls were grown on nickel nanoclusters with a diameter of approximately 100 nm in a reaction vessel within a quartz tube using a mixture of acetylene and nitrogen [80 SCCM (SCCM denotes cubic centimeter per minute at STP) $C_2H_2$ to 400 SCCM $N_2$], which flowed through the tube at a temperature of 700 °C for approximately 10 s. The nanopearls were formed only in the reaction vessel where the Ni catalyst was deposited.[7]

Carbon nanopearls were suspended in toluene at a concentration of 0.08 wt %. This solvent was selected based on previous experiments, where it was determined that toluene resulted in the most uniform and highest volume dispersion of nanopearls on the substrate.[5] The MAPLE deposition system and process for preparing MAPLE targets are described in detail elsewhere.[5]

For the MAPLE and MAPLE/magnetron sputtering experiments, a 248 nm KrF excimer laser source was focused onto a spot on the frozen target in a square pattern approximately 17.7 mm per side. The laser energy was 700 mJ/pulse and the repetition rate was 1 Hz. A magnetron sputter source with a 3.3 cm diameter gold target was operated at a power of 30–60 W. The processing gas flow rate and pressure in the vacuum chamber were regulated with individual mass flow controllers using a variable throttle valve. The proportion of oxygen to argon was varied while keeping the total flow rate fixed at 100 SCCM. The total chamber pressure was kept at 2.0–2.7 Pa during film growth.

Ion and neutral mass scans were conducted with a Hiden electrostatic quadrupole plasma (EQP) analyzer that allows measurement of the energy and mass distributions of ions, neutrals, or radicals generated in a source plasma. Early studies of sputtering and etching discharges using energy and mass analysis were performed by Coburn and Kay.[8,9] The key components comprising the EQP are the energy sector analyzer (ESA) and the quadrupole mass spectrometer (QMS). The ESA consists of two curved plates that are positively (outside plate) and negatively (inside plate) charged. Ions generated by the plasma enter the EQP but only those with a specific kinetic energy, for which the centrifugal and electrostatic forces are equal, can pass through the ESA and enter the secondary electron multiplier detector. Analysis of

neutrals can also be performed by activating an ionization source near the front sampling orifice.[10] The QMS consists of four cylindrical rods that produce a two-dimensional quadrupole by superimposing radio frequency (rf) and direct current (dc) potentials on the rods. When the rf and dc potentials are set to a certain critical ratio, only ions of a specific mass to charge ratio can pass through the rods to the secondary electron multiplier detector.[10]

Energy scans were performed for the primary species detected in the processes, which were generally neutral or singly ionized toluene, Ar, $O_2$, and O. Mass scans were subsequently performed at the most probable kinetic energy of the desired species measured with the analyzer as determined for each new condition. Since the incident laser was pulsed, the evolution of species from the target exhibited a strong time dependence on the microsecond scale. To account for this time dependence, a long dwell time (200 ms) for acquisition of spectra was selected. Multiple spectra were obtained at each condition and the results were averaged.

In order to compare the effects of oxygen to argon gas mixtures and other experimental conditions, it was necessary to measure the concentration of species detected by the EQP analyzer. This was accomplished using trapezoidal integration, with the assumption that the integrated area under a peak (or series of peaks) was proportional to the concentration of the species present within the processing system.

Gold-CNP hybrid films were deposited by MAPLE and magnetron sputtering codeposition at the following $O_2/Ar$ background gas ratios: 90 SCCM $O_2$/10 SCCM Ar, 20 SCCM $O_2$/80 SCCM Ar, and 75 SCCM $O_2$/25 SCCM Ar. Samples were characterized using scanning electron microscopy (SEM), high resolution TEM, and x-ray photoelectron spectroscopy (XPS).

The XPS analysis was performed using a Surface Science Instruments (SSI) M-probe XPS equipped with an Al $K\alpha$ x-ray source operated at a base pressure of approximately $4e^{-7}$ Pa. Spectra were analyzed using CASA XPS software, which has built-in corrections for spectrometer sensitivity factors for the SSI M-probe XPS. Au $4f_{7/2}$ and C $1s$ peak areas were measured using a Shirley background subtraction routine in order to compute the atomic percent of Au and C present on the surface. The samples were sputtered for 30 s using argon ions with kinetic energy (1 keV).

A gold-CNP hybrid film deposited using 75 SCCM $O_2$/25 SCCM Ar background gas was examined using SEM and a region of the surface containing embedded CNP clusters was selected for TEM analysis. A specimen was removed from this region by cutting a cross section with a focused ion beam (FIB) and then was examined using high resolution TEM.

## III. RESULTS AND DISCUSSION

### A. Argon background

Ion mass counts were monitored during operation of MAPLE in vacuum environment (base pressure $\sim 10^{-4}$ Pa) with no sputtering using the EQP analyzer. No ions were
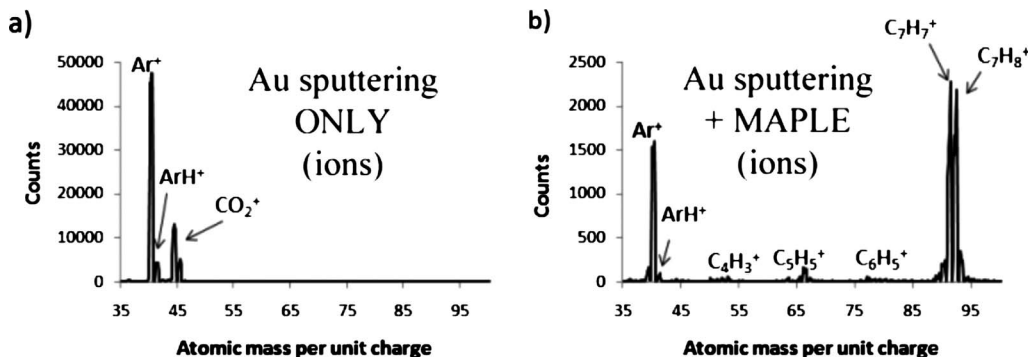
FIG. 1. Ion counts vs atomic mass per unit charge for (a) magnetron sputtering only (no MAPLE) with gold target and (b) magnetron sputtering with gold target operating and simultaneous MAPLE operation.

detected from the MAPLE process alone. During sputtering of gold in an argon background without MAPLE, argon ions were detected in abundance [Fig. 1(a)]. During sputtering in argon with MAPLE, argon ions were still present but their flux to the probe was significantly reduced [Fig. 1(b)]. In addition, ionized toluene and fragments were present.

The increased flux of ionized toluene species in the presence of argon during MAPLE is most likely due to ionization of the toluene by electrons generated from the magnetron.[11] However, the drastic decrease in argon ions compared to sputtering without MAPLE would suggest that charge exchange mechanisms between argon ions and neutral toluene species contribute to the total ion flux. These proposed reactions (e.g., $C_7H_8 + Ar^+ \rightarrow Ar + C_7H_8^+$) have a very high rate on the order of $10^{-10}$ cm$^3$/s.[12] The ionized and neutral toluene species form a solid carbon film on surfaces within the vacuum chamber, including the sputter target, which was visibly coated after 1–3 min of MAPLE and sputtering in argon. Ultimately, the deposition rate of carbonaceous species on the gold target was faster than the sputter rate of the target itself, resulting in deposition of thin amorphous carbon films with almost no gold content as the growth rate of carbon on the target was greater than the sputter rate (even at the 1 Hz laser repetition rate employed here), leaving the no exposed gold surface accessible to the incident argon ions. These processes are summarized in the schematic diagram shown in Fig. 2(a). Due to this illustrated carbon layer build-up on the sputter target surface the pure argon sputtering of gold combined with the MAPLE of CNPs from toluene based frozen targets was found not to be a suitable process for a preparation of CNP-gold composites.

## B. Oxygen background

The addition of oxygen to the process gas during magnetron-MAPLE codeposition was investigated in an effort to eliminate carbon deposition on the sputtering target. Removal of carbon from surfaces by reactive oxygen species is well documented and has been observed by previous researchers.[13–15] The efficacy with which the carbon was removed from surfaces within the chamber was observed qualitatively by depositing a carbon layer on the gold target by simultaneous MAPLE and magnetron sputtering in argon.

After growth of a visibly continuous carbon layer on the gold target, the laser and magnetron were shut off and the background gas was switched to oxygen. When the sputter process was reinitiated in the presence of oxygen, the surface of the gold target became visible, and the intensity of the plasma at the magnetron target increased. In addition, the neutral mass spectrum was monitored during this process and the concentrations of CO (28 amu) and $CO_2$ (44 amu) increased when the gas was switched to oxygen. The observed competition between carbon deposition and removal, which leads to significant reduced gold target surface contamination with carbon, is illustrated schematically in Fig. 2(b).

## C. Oxygen and argon background

Simultaneous MAPLE and magnetron sputtering experiments were conducted using mixtures of oxygen and argon
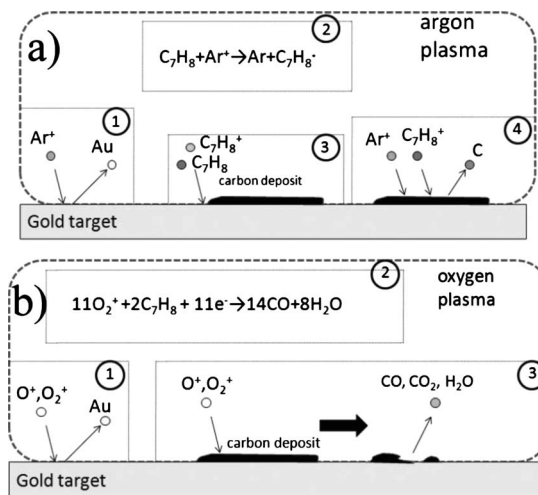


FIG. 2. (a) Mechanisms on a gold target surface in argon plasma during simultaneous MAPLE and magnetron sputtering: (1) sputtering of Au atoms in Ar plasma; (2) toluene/argon ion exchange; (3) deposition of carbon onto gold target surface; (4) sputtering of carbon from gold target surface. (b) Mechanisms in oxygen plasma during simultaneous MAPLE and magnetron sputtering: (1) sputtering of Au atoms in oxygen plasma; (2) example reaction of toluene vapor with oxygen plasma; (3) oxygen plasma reaction with carbon deposit on gold target surface
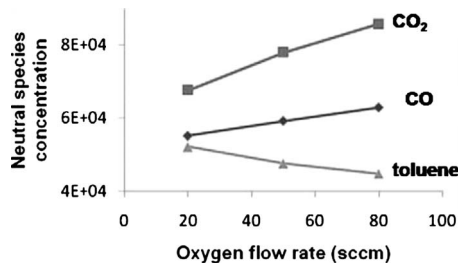
FIG. 3. Neutral species concentration vs oxygen flow rate (where oxygen flow rate+argon flow rate=100) during simultaneous magnetron sputtering with gold target operating and MAPLE operation.

as the background gas to minimize carbon deposits on the target and substrate surfaces while maximizing the sputter rate of gold. Mass spectra of neutral species were collected from 0 to 100 SCCM oxygen. Mass spectra for the ion species were collected from 88 to 97 amu; trapezoidal integration was used to compute the relative abundance of toluene in the vapor phase. For measurements of ion species, the gold target was cleaned by operating the magnetron in a pure oxygen background for 1 min between measurements for each gas mixture.

For the neutral species analysis, trapezoidal integration of the mass spectra was used to compute the relative abundance of atomic oxygen, carbon monoxide, carbon dioxide, and toluene. These areas were plotted versus oxygen flow rate. Mass spectra of neutral species showed the concentration of carbon monoxide and carbon dioxide increased with oxygen concentration while the flux of toluene decreased with increasing oxygen concentration (Fig. 3).

The effect of the oxygen to argon concentration ratio on the toluene ion concentration was also evaluated. Ionized toluene has characteristic major peaks at 91 amu ($C_7H_7^+$) and 92 amu ($C_7H_8^+$) as well as minor peaks at 93 and 94 amu. For the collected spectra, the toluene ion concentration was computed from 90 to 95 amu. The toluene ion concentration reached steady state after 4–5 min of deposition for all mixtures. Figure 4 shows the steady state toluene ion concentration versus the oxygen flow rate. The toluene ion concentration decreases with increasing oxygen flow rate, and for oxygen flow rates greater than 80 SCCM the toluene ion concentration becomes negligible (Fig. 4).
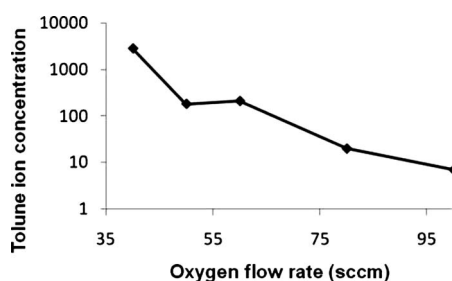


FIG. 4. Integrated toluene ion area (90–95 amu) vs oxygen flow rate during simultaneous magnetron sputtering with gold target operating and MAPLE operation.
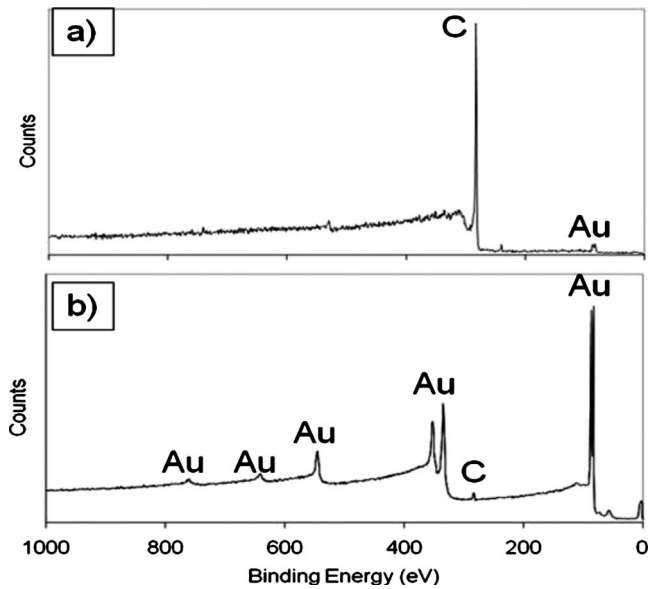


FIG. 5. XPS spectra of gold/carbon nanopearl hybrid films synthesized using simultaneous MAPLE and magnetron sputtering in (a) 100 SCCM Ar and (b) 90 SCCM $O_2$/10 SCCM Ar.

Based on processing regimes identified with the mass spectrometer, gold-carbon nanopearl composite films were synthesized using simultaneous MAPLE and magnetron sputtering on silicon substrates using two background gas mixtures, one at 20 SCCM oxygen, 80 SCCM argon and the other at 90 SCCM oxygen and 10 SCCM argon. All other deposition conditions were identical. The deposition rate for the 80 SCCM argon sample (20.0 nm/min) was over 2.5 times greater than that of the 10 SCCM argon sample (7.4 nm/min). This result was expected because the energy transfer, and therefore the sputter yield, between incident atomic ions on the gold target is reduced when oxygen is substituted for argon. This is largely due to the lower atomic mass of atomic oxygen and the fact that the effective kinetic energy for sputtering by molecular gases is reduced by a factor of 2 for incident molecular ions,[16] and small differences in kinetic energy can have a large effect on the sputtering yield, in the range 50–500 eV for gold targets.[17]

Samples synthesized by MAPLE and magnetron sputtering codeposition at different oxygen to argon ratios were characterized using XPS (Fig. 5). A sample that was deposited using 100 SCCM argon background contained mostly carbon (99.64 at. % C, 0.36 at. % Au) while a sample deposited using a background mixture of 90 SCCM oxygen and 10 SCCM argon contained both gold (56 at. %) and carbon (44 at. %). Note that due to very shallow electron escape depths (order of 20 nm) XPS analysis of gold-CNP composite films samples mostly gold matrix covering CNP clusters at the film surface, with a minimum signal from CNP particles themselves. The XPS results are in agreement with the proposed mechanism that carbon deposits are accumulated on and sputtered from gold target surfaces when using pure argon for sputtering combined with the MAPLE process (see Fig. 2). XPS data also confirmed that when oxygen background
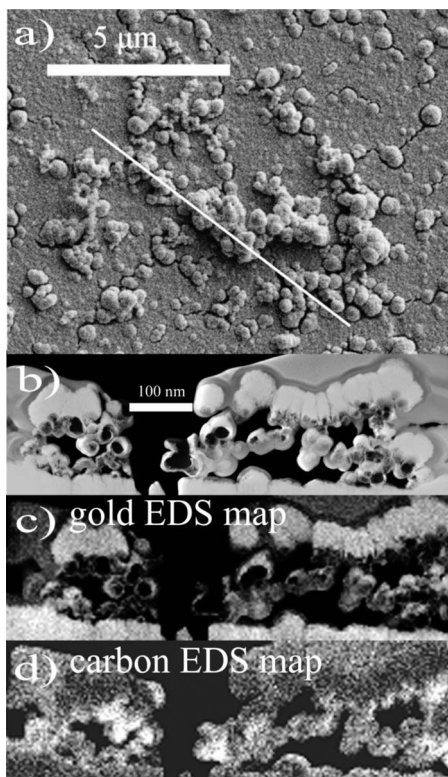
FIG. 6. (a) SEM micrograph of gold/carbon nanopearl hybrid film synthesized using simultaneous magnetron sputtering and MAPLE operation with 75 SCCM $O_2$/25 SCCM Ar background gas. The section removed for TEM analysis using the FIB is indicated by a white line in the micrograph. (b) TEM micrograph of gold/carbon nanopearl hybrid film synthesized using simultaneous magnetron sputtering and MAPLE operation with 75 SCCM $O_2$/25 SCCM Ar background gas. (c) EDS composition map for gold of region shown in (b). Gold intensity is proportional to the brightness. (d) EDS composition map for carbon of region shown in (b). Carbon intensity is proportional to the brightness.

gas is used in the deposition, the amount of amorphous carbon in the film is greatly reduced but is still present. MAPLE and magnetron sputtering codeposited sample surfaces were etched using an argon ion beam and the samples were examined using high resolution XPS and Auger spectroscopy in an attempt to distinguish between the carbon contained in CNPs and that deposited from other means (toluene vapor deposited or sputtered from the magnetron target surface). These techniques were unable to distinguish between these types of carbon. The reason for this is because while CNPs contain concentrically aligned graphitic flakes, they also contain amorphous carbon,[7] which prevented spectroscopic analysis discrimination of the carbon contaminant in gold matrices and in CNP nanostructures. Therefore, a film cross-sectional sample extraction with a FIB and TEM analysis with elemental composition mapping of carbon and gold was performed on the films produced by MAPLE-sputter process in a mixture of argon and oxygen as a background gas.

A SEM micrograph of surface morphology of the gold-CNP hybrid film deposited using 75 SCCM $O_2$/25 SCCM Ar background gas is shown in Fig. 6(a). A dotted line in Fig. 6(a) indicates the region containing embedded CNP clusters where the cross-sectional specimen was removed using the

FIB. A TEM micrograph of this specimen [Fig. 6(b)] shows that the film contains significant porosity adjacent to the CNP clusters. The porosity results from the fact that the MAPLE process deposits CNPs in clusters that act as masks for the gold atoms deposited by sputtering, preventing penetration between clusters. Figures 6(c) and 6(d) show energy dispersive spectrometry (EDS) composition maps for Au and C, respectively, of the region corresponding to the TEM micrograph in Fig. 6(a). The bright areas in Figs. 6(c) and 6(d) are regions with maximum counts of Au and C, respectively. A gold layer covers the top of the film and is distributed in the midst of the CNPs, consistent with the fact that the deposition processes occurred simultaneously. Carbon is concentrated mostly in the CNP clusters as expected but is distributed in lesser amounts throughout the surrounding gold matrix. This observation directly confirmed that carbon is incorporated in the gold film matrix by reaction between the toluene vapor from MAPLE and argon sputtering process.

Thus, the addition of oxygen to the sputtering background allowed the growth of gold-CNP composite films when using toluene solvent for MAPLE targets. However, it did not completely prevent the incorporation of carbon impurities originating from toluene into the gold matrix. The use of larger fractions of oxygen in the sputtering gas mixture may not be practical due to a large reduction in the sputtering efficiency.

Carbon impurities originating from toluene on sputter targets and deposited films could be reduced by other means. For example, solvents containing oxygen in the molecular structure [e.g., methanol, acetone, and dimethyl sulfoxide (DMSO)] could be used for the MAPLE target matrix. This would reduce the amount of additional oxygen in the sputtering background necessary to react with the carbon deposited from the matrix, although these solvents have been shown to produce a lower yield of solute material deposited via the MAPLE process.[5] Another possibility for examining the contribution of ionized and neutral toluene species is the use of an alternative background gas in place of argon to mitigate or eliminate the charge exchange process that generates toluene ions. Furthermore, charge exchange reactions of any kind could possibly be avoided by alternating magnetron sputtering and MAPLE processes rather than operating them at the same time. The later possibility seems to be more feasible based on results of the current studies, which show that such transfer occurs during simultaneous operation of MAPLE and magnetron sputtering. Typical durations of laser ablated plasma plumes are on the order of 0.01 ms, which are followed by order of 1 s delay time between the laser shots, which creates a good window opportunity for unaffected sputtering. Due to recent improvements in pulsed magnetron sputtering processes,[18] magnetron pulses can be easily synchronized with pulsed laser shots delivered to MAPLE targets to avoid hybrid plasma charge exchange reactions and prevent attraction of carbonaceous solvent ions to the metal sputtering surfaces. The residual solvent molecular presence in the chamber may be still a source of carbon impurities in deposited films, which may need to be investigated for use of synchronized pulsed plasma hybrid processes in the future.

## IV. CONCLUSIONS

A hybrid magnetron sputtering/MAPLE deposition process was investigated for growth of gold-CNP composite coatings. In the presence of pure argon, carbon deposits originating from toluene in the MAPLE target suppressed the sputtering of the magnetron target material, preventing growth of the desired composite film. Carbon deposits on a gold magnetron sputter target and carbon impurities in deposited films were observed while codepositing in pure argon. EQP analysis determined that ionization of toluene vapor generated from the MAPLE target was enhanced by charge exchange between neutral toluene molecules and argon ions generated in the presence of energetic electrons from the magnetron plasma. Carbon impurities of codeposited films were considerably reduced by using argon-oxygen mixtures as a background gas. This allowed for a growth of nanostructured composite films consisting of CNPs encapsulated in the gold matrix. However, carbon impurities were still present in the gold matrix as observed from XPS and cross-sectional TEM analysis for films grown at 75% oxygen fraction in the background gas. In addition, increasing the oxygen to argon ratio decreased the sputter yield of gold to the substrate over sputtering alone (e.g., without concurrent MAPLE deposition) in pure argon. This research has demonstrated that MAPLE and magnetron sputtering codeposition is a viable process for synthesizing composite films consisting of a nanoscopic phase produced outside the deposition process. Also, this research has established that charge transfer reactions in the MAPLE-sputtering hybrid plasma processes are responsible for solvent atom incorporation into the composite films, and several suggestions were proposed as mitigation alternatives for future developments of MAPLE based hybrid plasma processes.

[1] Andrew R. McGill, Douglas B. Chrisey, Alberto Pique, and Todd E. Mlsna, Proc. SPIE **3274**, 255 (1998).

[2] A. Piqué *et al.*, Thin Solid Films **355–356**, 536 (1999).

[3] A. Piqué, P. Wu, B. R. Ringeisen, D. M. Bubb, J. S. Melinger, R. A. McGill, and D. B. Chrisey, Appl. Surf. Sci. **186**, 408 (2002).

[4] B. Toftmann, K. Rodrigo, J. Schou, and R. Pedrys, Appl. Surf. Sci. **247**, 211 (2005).

[5] C. N. Hunter, M. H. Check, J. E. Bultman, and A. A. Voevodin, Surf. Coat. Technol. **203**, 300 (2008).

[6] M. Jelinek, T. Kocourek, J. Remsa, R. Cristescu, I. N. Mihailescu, and D. B. Chrisey, Laser Phys. **17**, 66 (2007).

[7] A. Levesque, Vu Thien Binh, V. Semet, D. Guillot, R. Y. Fillit, M. D. Brookes, and T. P. Nguyen, Thin Solid Films **464–465**, 308 (2004).

[8] J. W. Coburn and E. Kay, J. Vac. Sci. Technol. **8**, 738 (1971).

[9] J. W. Coburn and E. Kay, J. Appl. Phys. **43**, 4965 (1972).

[10] C. Muratore, "The influence of particle energy distributions on reactively sputtered titanium oxide and titanium nitride thin film compounds," Ph.D. dissertation, Colorado School of Mines, 2002.

[11] J. R. Vacher, F. Jorand, N. Blin-Simiand, and S. Pasquiers, Chem. Phys. Lett. **434**, 188 (2007).

[12] I. Ikezoe, S. Matsuoka, M. Takebe, and A. Viggiano, Gas Phase Ion-Molecule Reaction Rate Constants Through 1986, 1987.

[13] B. Landkammer, A. von Keudell, and W. Jacob, J. Nucl. Mater. **264**, 48 (1999).

[14] A. Cuesta, A. Martinez-Alonso, and J. M. D. Tascon, Carbon **39**, 1135 (2001).

[15] L. E. Cascarini de Torre, E. J. Bottani, A. Martinez-Alonso, A. Cuesta, A. B. García, and J. M. D. Tascón, Carbon **36**, 277 (1998).

[16] X. B. Tian, D. T. K. Kwok, P. K. Chu, J Appl. Phys. **88**(9), 4961 (2000)

[17] Y. Yamamura and H. Tawara, At. Data Nucl. Data Tables **62**, 149 (1996).

[18] J. G. Jones, C. Muratore, A. R. Waite, and A. A. Voevodin, Surf. Coat. Technol. **201**, 4040 (2006).